

MODEL CORRELATION PROCEDURES FOR AIR-CONDITIONING COPPER DISCHARGE TUBE

LIM DENG ZHAO¹, MOHAMMAD HOSSEINI FOULADI^{1,*},
YAP KIM HAW²

¹School of Engineering, Taylor's University, 47500, Subang Jaya, Selangor DE, Malaysia

²CAE/FEA, Panasonic Appliances Air-Conditioning R & D Malaysia Sdn Bhd
(PAPARADMY 1), 40300, Shah Alam, Selangor DE, Malaysia.

*Corresponding Author: hosseini@taylors.edu.my

Abstract

Investigations to perform complete Finite Element (FE) model correlation processes on Copper-Phosphorus multi-bent tubes in outdoor air-conditioning units were studied. This initiative is part of PAPARADMY 1's development plan in validating its FE models for more advanced CAE analysis to predict transient and random vibration response analysis. The Siemens PLM software's NX software was used to study the modelling, pre-test planning and correlation processes. Modal test data on the other hand was obtained from impact hammer tests using Bruel & Kjaer's Pulse. Several industrial metrics to evaluate results from each process were also presented to aid in correlation analysis. Both analytical and experimental natural frequencies showed good correlation with percentage error less than 5% for all mode pairs. Results from the Modal Assurance Criterion (MAC) showed reasonable correlation between experimental and numerical mode shapes with the maximum off-diagonal value being 0.3 and 7 highly correlated mode pairs were obtained. The complete workflows developed from this study is showcased in *Appendices A, B and C*.

Keywords: FEA, Modal Analysis, Pre-test, FE Model Correlation, Copper Tube.

1. Introduction

PAPARADMY 1 has undertaken a new development process to correlate FE models with modal test data. Correlation is a prerequisite for model validation which updates dynamic properties of FE models to closely represent physical prototypes. This initiative is to replace traditional design-to-production methods that are costly, time consuming and unsustainable. This can be achieved by incorporating

Nomenclatures	
A	Analytical modes (Work mode shapes)
i, j	Integer indices
$[K]$	Stiffness matrix
$[M]$	Mass matrix
N	Number of paired mode shapes
T	Experimental modes (Reference mode shapes)
x	Displacement vector, m
\ddot{x}	Acceleration vector, m/s ²
$[]^{-1}$	Inverse of a matrix
$[]^T$	Transpose of a matrix
Greek Symbols	
ψ	Eigenvectors
ω	Natural Frequency (Hz)
ω^2	Eigenvalues
Abbreviations	
AMA	Analytical Modal Analysis
CAD	Computer Aided Design
CAE	Computer Aided Engineering
COMAC	Coordinated MAC
CQUAD4	2D Quadrilateral Elements
DOF	Degree of Freedom
EMA	Experimental Modal Analysis
FE	Finite Element
FRF	Frequency Response Function
MAC	Modal Assurance Criterion
TAM	Test Analysis Model
2D	Two Dimensional
3D	Three Dimensional

advanced CAE analysis and reducing the number of built prototypes. However, model correlation needs to be performed beforehand to analyse the fidelity of existing FE models.

Vibration effects on air-conditioning piping systems have long been investigated with Yasuhiro and Tsutomu developing a set of manual for air-conditioning piping design using vibration analysis through optimizing Copper tube dimensions [1]. This initiative however, still relied upon a trial and error process until it passes the testing stages. In 2002, Ling proposed digital simulation techniques to predict vibration responses from air conditioners [2]. The focus then was centered upon the excitation from compressors and the effect on piping systems. The focus then shifted towards correcting piping designs through the use of frequency response as proposed by Manekshaw and Jassal [3]. The implementation of response analysis in the air-conditioning industry became possible when a boundary condition to test piping systems during operations was proposed by Chuan [4]. More recently, Loh et al. [5] presented a vibration

characteristic identification of piping systems using constrained testing methods. The aim was to assess the frequency predicted from numerical simulations and the operations of air-conditioning fan and compressors on the piping systems.

This research aims to identify the agreement between the dynamic characteristics of a Copper tube's FE model to its physical prototype with vibration loads during transportation. Modal data for the Copper tube has to be numerically predicted using NX Nastran. A modal test performed in a free-free boundary condition will be used to extract the actual dynamic properties of the prototype [6]. The two data sets will then be evaluated using existing industry metrics.

2. Description of the Structure

The multi-bent deoxidised Copper tube studied was a discharge tube used in a hermetic compressor that discharges compressed gas from the compressor housing. The tube model was part of a 1.5 Hp split-type outdoor air-conditioning unit. It consists of 11 bended sections with a circular cross section and a wall thickness of 7×10^{-4} m. A 3D CAD model of the tube and its assembly in an outdoor air-conditioning unit is shown in Fig. 1.

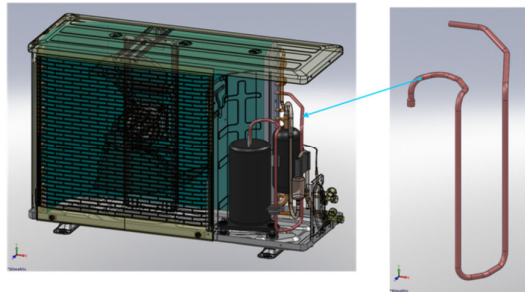


Fig. 1. 3D CAD Model of the Multi-bent Copper Discharge Tube and its Assembly in a 1.5 Hp Outdoor Air-Conditioning Unit.

3. Analytical Modal Analysis (AMA)

Basic dynamic properties of a structure are its natural frequencies and mode shapes which can be obtained through FE codes such as NX Nastran. AMA is solved in an undamped free vibration condition. A structure's equation of motion then takes the form in Eq. (1).

$$[M]\{\ddot{x}\} + [K]\{x\} = 0 \quad (1)$$

where $[M]$ = Mass matrix, $[K]$ = Stiffness matrix, \ddot{x} = Acceleration vector, and x = Displacement vector.

The solution to Eq. (1) takes the form of Eq. (2) as harmonic motion is assumed and yields an eigenvalue problem Eq. (3). The Lanczos method is then used to extract a set of eigenvalues (ω^2) and eigenvectors (ψ) that corresponds to the structure's natural frequencies and mode shapes respectively. An important assumption in modal analysis is that the structure is linear and time-invariant [7].

$$\{x\} = \{X\}e^{i\omega t} \tag{2}$$

$$-\omega^2 [M]\{X\} + [K]\{X\} = 0 \tag{3}$$

A set of natural characteristics of the Copper discharge tube was obtained computationally through Siemens PLM Software’s NX Nastran. The Sol 103 solver for normal modes analysis was used to obtain the tube’s natural frequencies and mode shapes. This forms the pre-requisite for model correlation as the analytical results obtained are to be verified against experimental results through EMA.

The Copper tube was modelled using 2D CQUAD4 shell elements with C10100 Copper which has a Young’s modules of 114 GPa and Poisson’s ratio of 0.31. The selections of 2D elements were due to bad bending behaviour and stiffer elements behaviour of 3D elements [8]. A total of 24,632 CQUAD4 elements were created with a mesh size of 1 mm. Solver parameters were then set for 1 Hz to 300 Hz based on Panasonic’s transportation vibration specification. The reason for 1 Hz selection was to avoid the extraction of rigid body modes. The last step was setting the eigenvalue extraction method to Lanczos and the solver was started. A total of 10 modes within the frequency range of interest were extracted and are shown in Fig. 2.

Modes 1, 4, 5 and 10 showed first, second, third and fourth bending modes in the Z-DOF respectively. Modes 2, 3, 7 and 8 on the other hand showed first, second, third and fourth torsion modes in the Y-Z plane. Finally, modes 6 and 9 show the first and second torsional modes in the X-Z plane. As the requirements for this stage of the study was to implement correlation analysis, all ten modes were considered for the following stages of pre-test planning and FE model correlation.

4. Pre-test Planning

4.1. Sensor measurement location

Pre-test planning is a process where the sensor locations and a representative model known as TAM are created. The Min-MAC (Minimum MAC) algorithm is an automated procedure that locates the best positions to place sensors to lower off-diagonal terms in an AutoMAC (Automatic MAC) matrix [9]. The AutoMAC matrix is used as the validation tool for sensor placement and it consists of a square matrix which correlates a set of mode shapes to itself. Therefore, the diagonal values (identical mode pairs) will always be unity, 1, leaving the off-diagonal terms with scaled values ranging from 0 to 1, to check if the mode shapes within the frequency range of interest could be captured and distinguished clearly. The ideal results for an AutoMAC matrix is that all off-diagonal terms should be lower than 0.1. The AutoMAC matrix is calculated based on Eq. (4).

$$AUTOMAC(A_1, A_2) = \frac{\left| \sum_{j=1}^N \psi_{A_1j} \psi_{A_2j}^* \right|^2}{\sum_{j=1}^N \psi_{A_1j} \psi_{A_1j}^* \sum_{j=1}^N \psi_{A_2j} \psi_{A_2j}^*} \tag{4}$$

where $\psi_{A_1j} = j^{th}$ value of mode ψ_{A_1} , $\psi_{A_2j} = j^{th}$ value of mode ψ_{A_2} and $\psi^* =$ complex conjugate value.

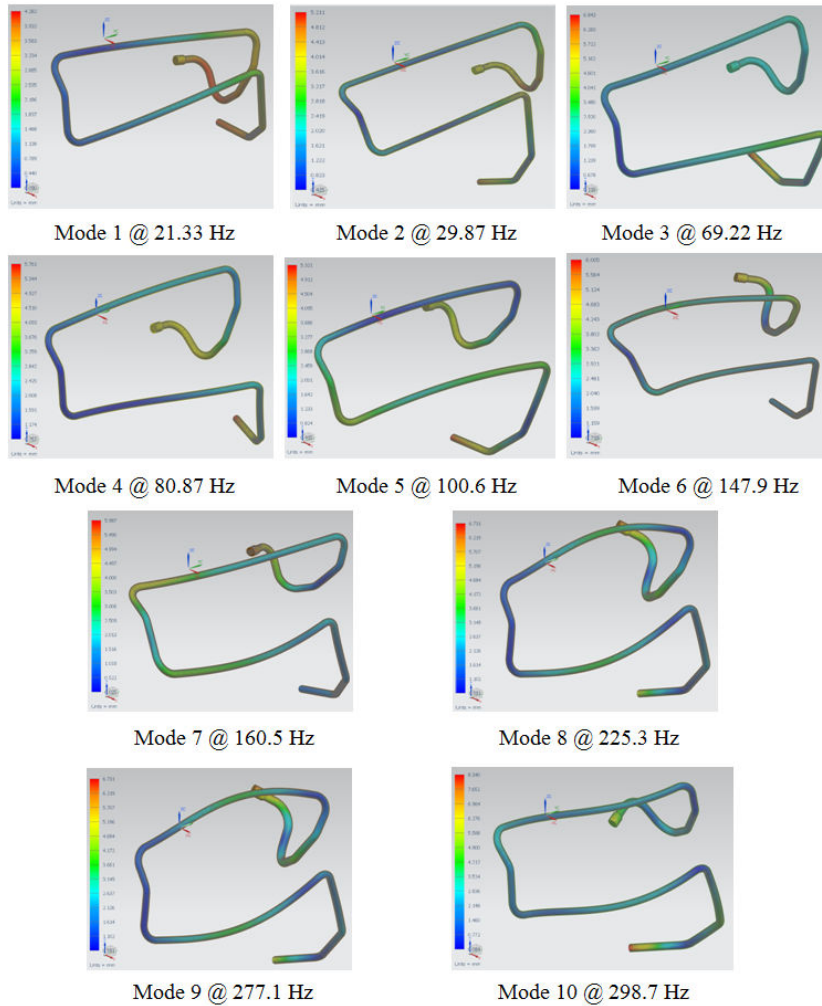
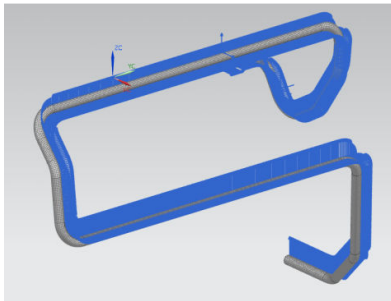


Fig. 2. Ten Mode Shapes Obtained from NX Nastran Sol 103 for 1 to 300 Hz.

The selection of sensor locations relies upon a trial and error process in NX Pre-test planning and consists of three main stages. First, a candidate group of possible sensor placement positions were selected. Its corresponding translational DOFs were then activated. For candidate set DOFs, only node points that are accessible during modal testing are selected. The next step requires the selection of at least two DOFs for measurement. These DOFs are usually selected at the free ends of the structure where the displacements are high. The third stage is where the Min-MAC algorithm is utilised to determine optimum sensor locations for pre-defined number of sensors to be used. The configurations are then assessed through the AutoMAC matrix to evaluate if all mode shapes within the frequency range of interest could be captured and clearly distinguished. If the

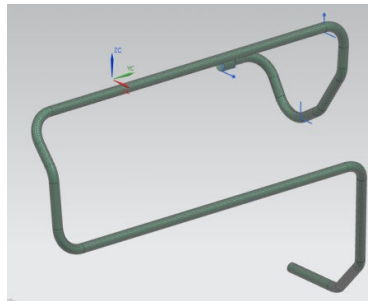
desired Auto-MAC results are not achieved, the second and third stages are to be repeated until the best configuration possible is obtained.

For the Copper discharge tube used in this study, a total of 2107 DOFs were selected as candidate positions for testing. By analysing the normal modes from Fig. 2, three required DOFs were selected at nodes 24472, 23431 and 23481 for X, Y and Z DOFs respectively as shown in Fig. 3. Since only seven uni-axial accelerometers were available for testing, the Min-MAC algorithm was solved for seven sensors and the proposed seven measurement points are shown in Fig. 4. The corresponding Auto-MAC matrix was plotted and shown in Table 1. Although 3 mode pairs (A2, S6), (A3, S10) and (A4, S9) showed relatively high off-diagonal values, the configuration was accepted based on the notion of insufficient number of accelerometers available for modal testing. These values would be checked upon correlation and compared if they do cause poor correlation results.



3(a)

Fig. 3(a) Candidate DOFs selection on Copper Tube.



3(b)

Fig. 3(b) 3 required DOFs selected on Copper Tube.

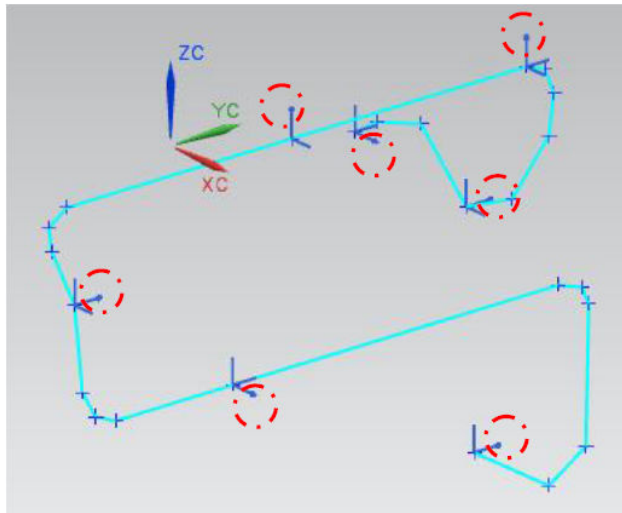


Fig. 4. Seven Measurement Points Proposed based on the Min-MAC Algorithm.

Table 1. AutoMAC Plot for Proposed 7 Sensors and its Corresponding Grey Scale. A refers to Analysis Modes (FE model), and S refers to Sensors Acquired Modes (7 Measurement Points).

	A1	A2	A3	A4	A5	A6	A7	A8	A9	A10	Scale
S1	1.0	0.2	0.1	0.0	0.0	0.1	0.2	0.1	0.2	0.0	0.1
S2	0.2	1.0	0.2	0.1	0.2	0.3	0.0	0.0	0.0	0.0	0.2
S3	0.1	0.2	1.0	0.1	0.0	0.1	0.0	0.0	0.2	0.3	0.3
S4	0.0	0.1	0.1	1.0	0.0	0.0	0.1	0.1	0.3	0.2	0.4
S5	0.0	0.2	0.0	0.0	1.0	0.2	0.1	0.1	0.0	0.1	0.5
S6	0.1	0.3	0.1	0.0	0.2	1.0	0.0	0.0	0.2	0.1	0.6
S7	0.2	0.0	0.0	0.1	0.1	0.0	1.0	0.0	0.2	0.0	0.7
S8	0.1	0.0	0.0	0.1	0.1	0.0	0.0	1.0	0.2	0.1	0.8
S9	0.2	0.0	0.2	0.3	0.0	0.2	0.2	0.2	1.0	0.0	0.9
S10	0.0	0.0	0.3	0.2	0.1	0.1	0.0	0.1	0.0	1.0	1.0

4.2. TAM derivation

TAM is the geometry used for modal testing. It represents the characteristics of the structure but with limited DOFs. This simplifies the test structure and saves time by only exciting or measuring critical DOFs. TAM can be created through manual selection of a structure's wireframe. The effectiveness of a TAM to represent its FE model's dynamic characteristics can be verified by performing an analysis-analysis correlation. The MAC metric and frequency difference plot are used to verify the TAM's effectiveness.

The MAC is an alternate form of the AutoMAC with differences being the correlated data sets. It is the most widely used metric to evaluate the quality of correlation. When verifying a TAM, the MAC is used to compare two sets of modal data solved analytically with the fully meshed model being used as the reference. The MAC is calculated using Eq. (5). Acceptable MAC values are that its diagonal terms should be more than 0.8 or 0.9 depending on the analyst and its off-diagonal terms lower than 0.1.

$$MAC(A,T) = \frac{\left| \sum_{j=1}^N \psi_{Tj} \psi_{Aj}^* \right|^2}{\sum_{j=1}^N \psi_{Tj} \psi_{Tj}^* \sum_{j=1}^N \psi_{Aj} \psi_{Aj}^*} \quad (5)$$

where N = number of paired mode shapes between two sets of modal data, ψ_T = reference mode shapes (mode shapes obtained from the FE model), ψ_A = work mode shapes (mode shapes obtained from reduced DOFs model) and ψ^* = complex conjugate value.

An initial configuration was created by selecting nodes that fully represent the tube's wireframe. A set of 24 nodes were selected to represent the tube wireframe as opposed to the original 25226 nodes for the full FE model. An analysis-analysis correlation was then performed to evaluate the adequacy of 24 nodes representing the Copper tube during testing. The derived TAM model is shown in Fig. 5 and the corresponding MAC plot for is shown in Table. 2.

Table 2. Analysis-Analysis Correlation MAC Plot for TAM and its Corresponding Grey Scale. R refers to Reference Modes (FE Model), and W refers to Work Modes (TAM Model).

	R1	R2	R3	R4	R5	R6	R7	R8	R9	R10	Scale
W1	1.0	0.0	0.0	0.1	0.0	0.1	0.0	0.0	0.0	0.0	0.1
W2	0.0	1.0	0.0	0.0	0.0	0.1	0.0	0.0	0.0	0.1	0.2
W3	0.0	0.0	1.0	0.0	0.0	0.1	0.1	0.1	0.0	0.1	0.3
W4	0.1	0.0	0.0	1.0	0.0	0.0	0.0	0.1	0.1	0.2	0.4
W5	0.0	0.0	0.0	0.0	1.0	0.0	0.1	0.2	0.0	0.0	0.5
W6	0.1	0.1	0.1	0.0	0.0	1.0	0.0	0.0	0.0	0.1	0.6
W7	0.0	0.0	0.1	0.0	0.1	0.0	1.0	0.0	0.1	0.0	0.7
W8	0.0	0.0	0.1	0.1	0.2	0.0	0.0	1.0	0.0	0.0	0.8
W9	0.0	0.0	0.0	0.1	0.0	0.0	0.1	0.0	1.0	0.0	0.9
W10	0.0	0.1	0.1	0.2	0.0	0.1	0.0	0.0	0.0	1.0	1.0

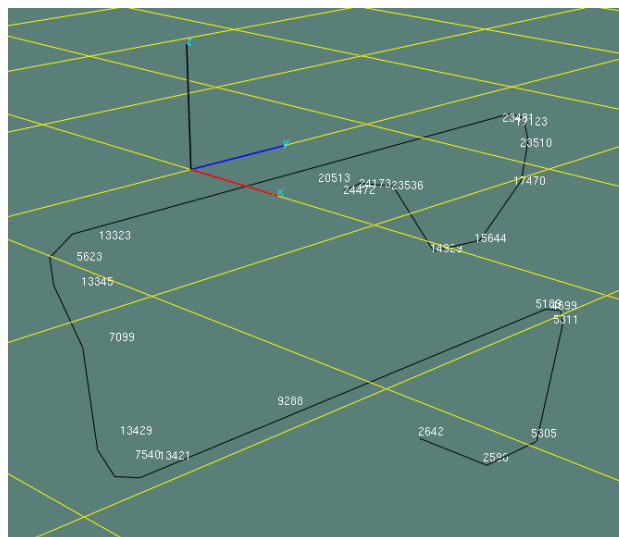


Fig. 5. TAM Representation of the Copper Discharge Tube.

5. Experimental Modal Analysis

The following sections present the measurement verification procedure before model correlation was performed. These checks are required to ensure that the potential errors arising from modal test are mitigated as much as possible. When these verification procedures are met, the data can then be exported for correlation.

5.1. Test setup

The test condition employed was to simulate “free-free” boundary conditions as close as possible. For correlation of individual components, the modal tests performed on this boundary condition would yield the best results [10]. Figure 6

shows the "free-free" boundary condition employed for the Copper tube during testing. An elastic chord was used to hang the Copper tube at presumed nodal points based on AMA results.



Fig. 6. Free-Free Test Setup of Copper Discharge Tube.

Once the specimen was setup, the verification process continued with checking settings defined on the analyzer. Parameters that need verification were lines of resolution, frequency range, averaging domain and analysis mode. Figure 7 shows the analysis setup window in Bruel & Kjaer's Pulse Modal Test Consultant.

Span is checked for the intended frequency range to be correlated with FE models are properly specified. Lines of resolution allow the user to specify how clearly measured response can be viewed. When closely spaced modes are anticipated, clearer lines of resolution are required. Averaging on the other hand, is used to minimize noise measurements. For modal tests, spectrum averaging is used as it clearly distinguishes the measured natural frequencies and noise. In this case, the number of averages was set to 5, so that consistency error can be minimized. This test was performed with an impact hammer, therefore a transient window was applied and response signals were weighted with exponential windows [11].

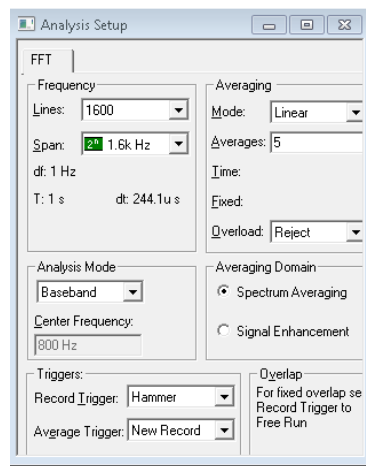


Fig. 7. Analysis Setup in Bruel & Kjaer's Pulse MTC Hammer.

5.2. Measurement check

Measurements are normally checked for a property known as coherence. Coherence is a scalar graph from 0 to 1 that shows the reproducibility of measured FRFs. A coherence value of close to 1 is always desired. Figures 8(a) and (b) show an example of a FRF and its corresponding coherence function for measurement point (242642 Y+, 224472 Z+). The drive point measurements are also an important verification procedure. These are measurement points where both sensor and impact points coincide. An important characteristic for drive point measurements are that the anti-resonance peaks follows every peak as shown in Fig. 9. Good quality drive point measurements allows for better synthesis of overall FRF data.

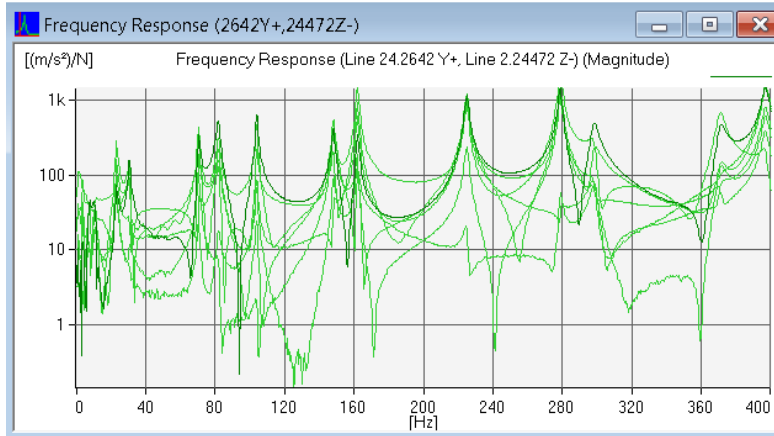


Fig. 8(a). Sample FRF Measurements after 4 Averages.

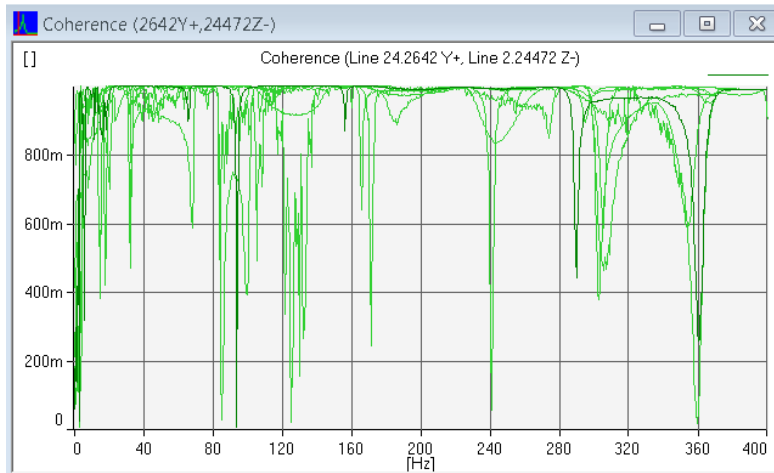


Fig. 8(b). Sample of Coherence Plot from the 4 Averages Measured.

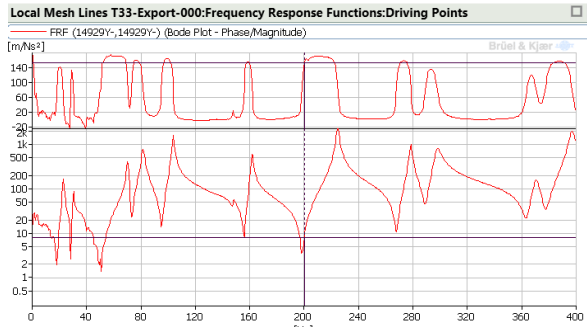


Fig. 9. Drive Point Measurement Verified for the Copper Discharge Tube Test.

5.2. Parameter estimation

All measurements were then exported into Pulse Reflex where measured FRFs and the structure’s modal data can be extracted. This verification stage assesses the curve-fitting method employed for modal data extraction. For this study, the RFPZ method was employed [12] and the corresponding mode table in Table 3 was obtained. A final verification of bode plot was checked to ensure that the mode table data were normalised. An important property of normal modes is that its phase differences are concentrated in 0 and 180 degrees as shown in Fig. 10. Results from modal testing are shown in Fig. 11.

Table 3. Dynamic properties extracted from test data after curve fitting.

No.	Natural Frequency (Hz)	Damping Ratio (%)	Complexity	Extraction Method
1	22.74143	0.82005	0	RFPZ
2	30.28512	2.22183	0	RFPZ
3	70.12834	0.75352	0	RFPZ
4	81.31347	1.30641	0	RFPZ
5	103.52491	0.62005	0	RFPZ
6	147.79208	0.51701	0	RFPZ
7	161.88902	0.23377	0	RFPZ
8	224.60641	0.37918	0	RFPZ
9	278.32158	0.31356	0	RFPZ
10	297.74545	0.80707	0	RFPZ

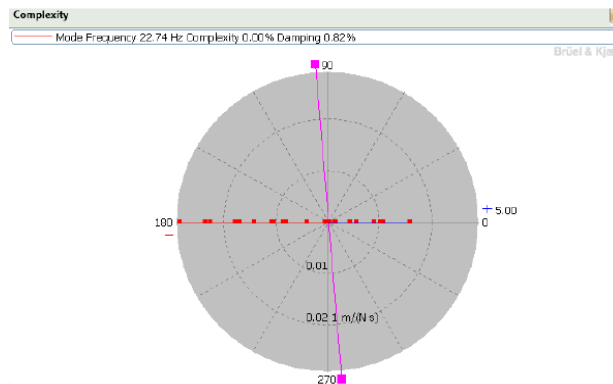


Fig. 10. Bode Plot Showing that Mode 1 has been Normalised.

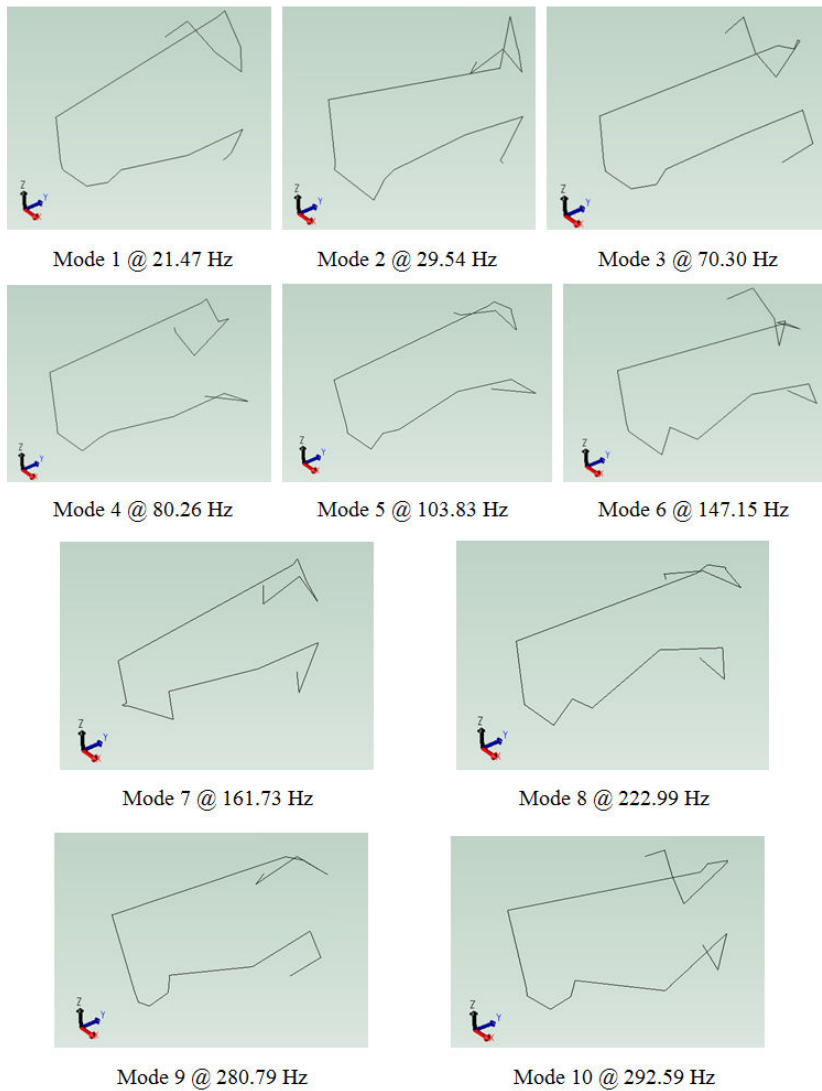


Fig. 11. Ten Modes Obtained from Modal Testing.

6. FE Model Correlation with NX Nastran

Model correlation assesses the degree of agreement between two sets of modal data. NX FE Model Correlation provides analysis-analysis correlation and test-analysis correlation. The quality of correlated modal data is assessed through modal vector correlation and DOF correlation. Modal vector correlation measures the vector displacement of calculated mode shapes. This provides a global indicator on the quality of the correlation. DOF correlation checks a system's

individual DOFs contribution towards the overall vector correlation. A frequency check is employed to assess the percentage error of derived natural frequencies.

The principal metric used in correlation is the MAC. It assesses the degree of linearity between two sets of mode shape vector. This degree of linearity is determined by a range of scalar value between 0 and 1. To obtain a scalar value, the MAC normalizes the magnitude of the mode shape vectors. MAC value of 1 indicates a well correlated set of mode shapes. MAC value of 0 then indicates poor correlation. The COMAC helps identify the local DOFs within a structure that produces low degree of correlation. Like the MAC, the COMAC metric also unit-normalizes the mode shapes. Values of 0 indicate a DOF that has poor correlation. COMAC of 1 indicates high correlation at a particular DOF. In NX, the COMAC can only identify low correlation DOFs only if mode pairs were selected. COMAC is calculated using Eq. (6). The COMAC is also represented in a graphically as the 1-COMAC. Equation 7 shows the calculation of the 1-COMAC.

$$COMAC(j) = \frac{\left(\sum_{i=1}^L \psi_{Tij} \psi_{Aij} \right)^2}{\sum_{i=1}^L \psi_{Tij}^2 \sum_{i=1}^L \psi_{Aij}^2} \quad (6)$$

$$1 - COMAC(j) = 1 - \left\{ \frac{\left(\sum_{i=1}^L \psi_{Tij} \psi_{Aij} \right)^2}{\sum_{i=1}^L \psi_{Tij}^2 \sum_{i=1}^L \psi_{Aij}^2} \right\} \quad (7)$$

where $j = j^{\text{th}}$ degree of freedom, ψ_{Tij} = mode shape of test data set with mode pair i , and ψ_{Aij} = mode shape of analytical data set with mode pair i .

Prior to running correlation analysis with NX FE Model Correlation, test data needs to be imported. The next step would be to identify mode pairs with options such as automatic pairing by MAC, sequential mode pairing or manual mode pairing. This step is essential if the 1-COMAC metric is to be used for post-processing. The workflow for correlation analysis is shown in *Appendix C*.

6.1. Frequency check

The natural frequencies extracted from modal test data were compared to computational results obtained from NX Nastran Sol 103 solver. The results are presented in Table 4 and percent error was calculated using Eq. (8).

$$PercentError(\%) = \left| \frac{\omega_{Test} - \omega_{Numerical}}{\omega_{Test}} \right| \times 100\% \quad (8)$$

6.2. MAC

The correlation MAC plot is presented in Table 5.

Table 4. Comparison of natural frequencies from AMA and EMA.

Mode No.	Natural Frequencies (Hz)		% Difference
	AMA	EMA	
1	21.33	21.47	0.65
2	29.87	29.54	-1.12
3	69.22	70.3	1.54
4	80.87	80.26	-0.76
5	100.6	103.83	3.11
6	147.9	147.15	-0.51
7	160.5	161.73	0.76
8	225.3	222.99	-1.04
9	277.1	280.79	1.31
10	297.8	292.59	-1.78

Table 5. Correlation MAC Plot and its Corresponding Grey Scale. R refers to Reference Modes (Modal Test), and W refers to Work Modes (AMA).

	R1	R2	R3	R4	R5	R6	R7	R8	R9	R10	Scale
W1	0.2	0.0	0.1	0.1	0.0	0.0	0.0	0.0	0.0	0.0	0.1
W2	0.5	0.9	0.1	0.0	0.0	0.0	0.1	0.0	0.2	0.0	0.2
W3	0.1	0.1	0.8	0.0	0.1	0.1	0.1	0.2	0.0	0.0	0.3
W4	0.1	0.1	0.0	0.9	0.0	0.0	0.0	0.0	0.0	0.0	0.4
W5	0.0	0.0	0.0	0.0	0.6	0.0	0.0	0.1	0.0	0.3	0.5
W6	0.0	0.0	0.0	0.0	0.0	0.3	0.3	0.1	0.0	0.0	0.6
W7	0.1	0.2	0.1	0.0	0.0	0.1	0.9	0.1	0.0	0.1	0.7
W8	0.0	0.0	0.3	0.0	0.0	0.1	0.1	0.8	0.0	0.2	0.8
W9	0.0	0.0	0.0	0.1	0.0	0.0	0.0	0.0	0.1	0.0	0.9
W10	0.0	0.1	0.1	0.0	0.1	0.1	0.2	0.4	0.1	0.6	1.0

6.3. Auto-MAC

The MAC plot showed poor correlation for modes 1, 6 and 9. The 1-COMAC was then used to identify local DOFs that contributed towards this error. Fig. 12 (a), (b) and (c) shows the 1-COMAC plots for X, Y and Z DOF respectively.

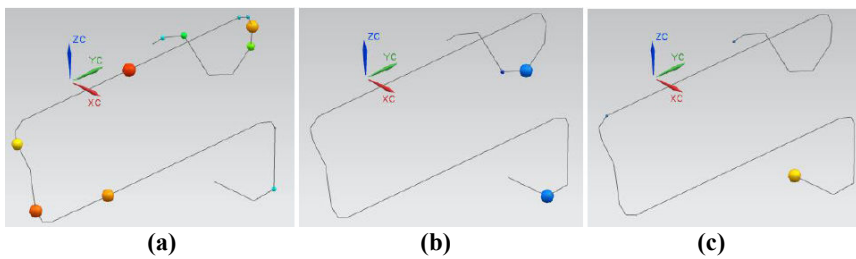


Fig. 12. 1-COMAC Plots for X, Y and Z DOFs respectively.

7. Discussions

The results above showed that mode shape vectors correlated poorly in the X DOF while natural frequencies showed very good data. This means the material properties employed in numerical analysis were accurate in predicting natural frequencies. A visual comparison of the poorly correlated mode pairs showed that the mode shapes extracted from modal test had sharp bending edges.

Assessment of the off-diagonal values in Table 5 showed that three mode pairs (R1, W2), (R3, W8) and (R8, W10) were not clearly distinguished. From the Auto-MAC results in Table 1, these were not identified through the pre-test planning stage. On the other hand, the earlier concerns for mode pairs (R2, W6), (R3, W10) and (R4, W9) showed that measurements were clearly distinguished. More configurations of sensor locations are therefore needed before the final 7 points for measurement can be clearly determined.

From the 1-COMAC plot, the 4 X direction DOF sensors around the U bend causes the lowest correlation values. The sensors were then deactivated to check if the diagonal MAC values improved. This is illustrated in Table 6. Compared to Table 5, the new MAC plot showed better correlation for mode pair 6. However, several off-diagonal values increased in value and mode pairs 1, 6 and 9 still do not correlate, with values below 0.8. This is still an unacceptable MAC plot.

Table 6. Correlation MAC Plot after Deactivating 4 Sensors and its Corresponding Grey Scale. R refers to Reference Modes (Modal Test), and W refers to Work Modes (AMA).

	R1	R2	R3	R4	R5	R6	R7	R8	R9	R10	Scale
W1	0.2	0.0	0.0	0.2	0.0	0.0	0.0	0.0	0.1	0.0	0.1
W2	0.5	0.9	0.1	0.0	0.0	0.1	0.0	0.0	0.3	0.0	0.2
W3	0.1	0.1	0.9	0.0	0.1	0.1	0.1	0.2	0.0	0.0	0.3
W4	0.1	0.0	0.0	0.9	0.0	0.0	0.0	0.0	0.0	0.0	0.4
W5	0.0	0.0	0.0	0.0	0.8	0.0	0.0	0.1	0.0	0.3	0.5
W6	0.0	0.1	0.0	0.0	0.0	0.4	0.3	0.1	0.0	0.0	0.6
W7	0.1	0.1	0.2	0.0	0.0	0.1	0.9	0.1	0.0	0.1	0.7
W8	0.0	0.0	0.4	0.0	0.0	0.1	0.1	0.8	0.0	0.3	0.8
W9	0.0	0.1	0.0	0.1	0.0	0.0	0.0	0.0	0.2	0.0	0.9
W10	0.0	0.1	0.1	0.0	0.2	0.1	0.2	0.4	0.1	0.7	1.0

Since deactivating the response of the 4 DOFs does not yield any significant improvement, the errors are then focused upon modal test data. Modal test data were verified to have been measured well with optimal coherence functions. However, further investigation revealed that only a single accurate drive point measurement was obtained. Besides, poor correlation could have been caused by test setup errors. The only way to verify is to check the FRFs of the test data for any abnormal peaks besides mode shapes. Smaller peaks could indicate an interference with the Copper tube hanging points [11]. Another cause of concern was that the hanging points of the bungee cords during testing. Improper hanging points could induce or affect the localised stiffness and damping properties of the structure [13]. Last but not least, a relatively quiet environment is needed during modal test to

prevent noise measurements. This was not always the case as the test environment during the Copper discharge tube test was constantly affected by random noises.

The current study has shown that a good correlation analysis is fully relied upon the accuracy of modal test data as numerical methods have been well established especially in the cases of light structures. The current research work is focused upon developing the processes related to FE model correlation and further investigations are required to analyse causes for poor correlation. A further study on designing modal test for Copper tubes is needed before correlation of sub-assembly for piping systems are considered.

8. Conclusions

The complete processes of numerical modelling, analytical modal analysis, modal pre-test planning and correlation stages were investigated using Siemens PLM software's NX. The complete workflows were successfully developed and implemented on a Copper discharge tube of a split-type outdoor air-conditioning unit. The following concluding remarks were made from this investigation.

- Pre-test planning helps identify critical measurement points accurately and helps simplify the modal testing phase by eliminating uncertainties related to data measurement errors and structures with inconsistent geometry.
- The material properties used for Copper tubes are accurate due to the closeness of natural frequencies obtained numerically and experimentally.
- Mode shape vectors were not successfully correlated as the MAC showed acceptable values for only 7 modes. Further investigations into impact hammer testing methods are required to complete the correlation analysis of Copper discharge tubes.

Acknowledgements

Special thanks are directed to PAPANADMY 1 Deputy Director Mr. Low Seng Chok for the approval and procurement of Copper discharge tubes for testing. The authors are also indebted to Mr. Cheng Chee Mun, General Manager of the Cost Management Department (CMD) for authorising the use of FEA-Project Team's NX CAE Software and B&K test equipment.

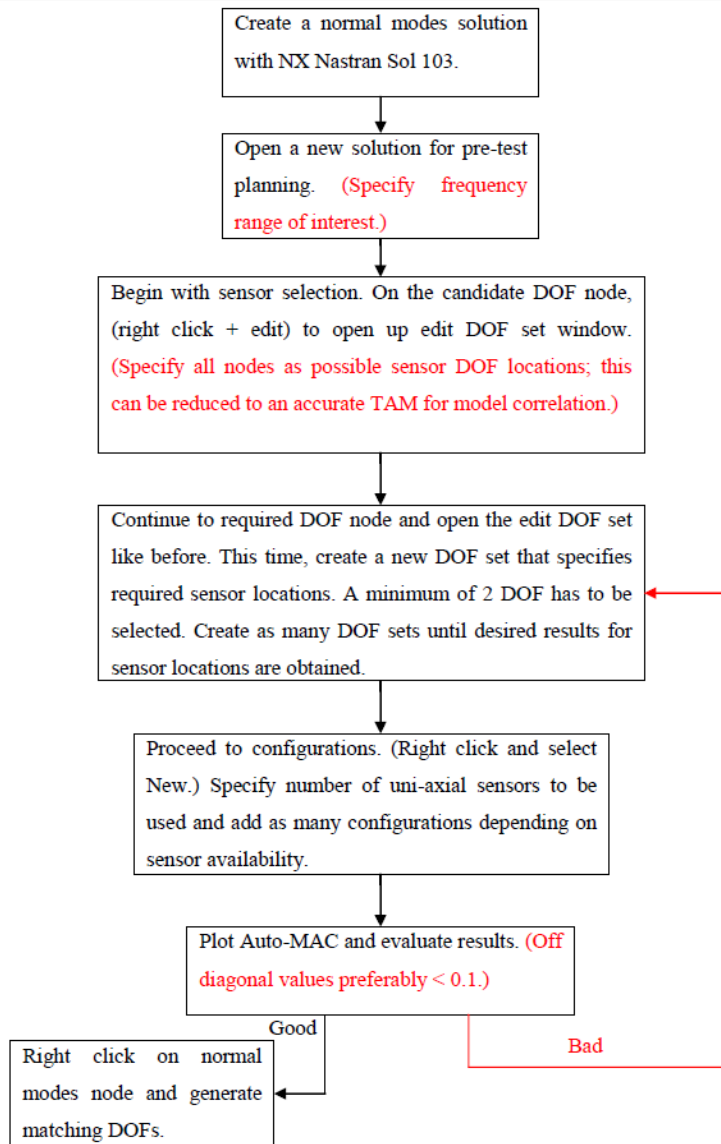
References

1. Yasuhiro, A.; and Tsutomu, S. (2001). Development of vibration analysis for piping design. *Nippon Kikai Gakkai Kansai Shibu Teiji Sokai Koenkai Koen Ronbunshu*, 76(1), 10.21-10.22.
2. Ling, J. (2002). The digital simulation of the vibration of compressor and pipe system. *International Compressor Engineering Conference*. Indiana, U.S.A, 1567.
3. Manekshaw, A.; and Jassal, A. (2001). Optimization of air-conditioner copper tube layout for frequency response. *Application note*. Altair Engineering, India.

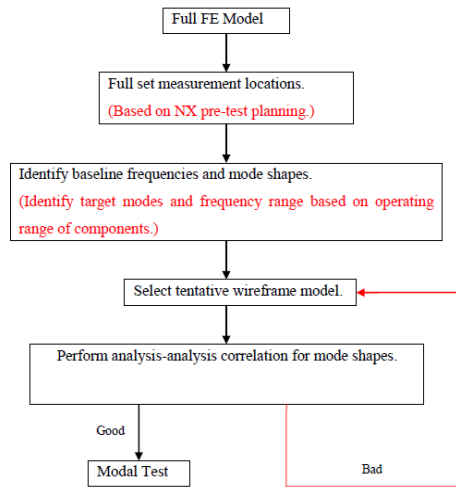
4. Chuan, X.D.; and Guang, M. (2007). Determining the boundary conditions by estimating RDOFs CMS for piping system. *Journal of Building and Environment*, 42(7), 2660-2666.
5. Loh, S.K.; Faris, W.F.; Hamdi, M.; and Chin, W.M. (2011). Vibrational characteristic of piping system in outdoor air-conditioning unit. *Science China Technological Sciences*, 54(5), 1154-1168.
6. Perinpayanagam, S.; and Ewins, D.J. (2003). Free-free, fixed or other test boundary conditions for the best modal test? *Proceedings of the 21st International Modal Analysis Conference*. Florida, U.S.A.
7. He, J.; and Fu, Z.F. (2001). *Modal Analysis*. (1st Ed.). London: Butterworth-Heinemann.
8. Allemang, R.J.; and Brown, D.L. (1982). A correlation coefficient for modal vector Analysis. *Proceedings of the 1st International Modal Analysis Conference*. Florida, U.S.A.
9. Ren, W.; Peng, X.; and Lin, Y. (2005). Experimental and analytical studies on dynamic characteristics of a large span cable-stayed bridge. *Journal of Engineering Structures*, 27(4), 535-548.
10. Richardson, M.; and Schwarz, B. (2003). Modal parameter estimation from operating data. *Sound and Vibration Magazine*, 37(1), 28-36.
11. Urbina, A.; Paez, T.L.; Rutherford, B.; O'Gorman, B.; Hinnerichs, T.; and Hunter, P. (2005). Validation of mathematical models: An overview of the process. *Proceedings of the SEM Conference and Exposition on Experimental and Applied Mechanics*. South Carolina, U.S.A.
12. Mayes, R.L. (1997). A tool to identify parameter errors in finite element models. *Proceedings of the 15th International Modal Analysis Conference*. Florida, U.S.A.
13. Ashory, M.R. (1999). *High quality modal testing methods*. Ph.D. dissertation. Imperial College of Science, Technology and Medicine, London, U.K.

Appendix A

Sensor Measurement Workflow



Appendix B TAM Derivation Workflow



Appendix C Model Correlation Workflow

